On-Command Pyrotechnic Light, Color, and Temperature Enhancement through Microwave Irradiation

Stuart J. Barkley, *[a] Ryan Ogorzalek, [a] William F. Crespo, [a] Jonathan M. Dilger, [a]
James B. Michael, [b] Travis R. Sippel [b]

[a] NSWC Crane, Indiana 47522
[b] Iowa State University, Iowa 50011

*corresponding author e-mail: stuart.j.barkley.civ@us.navy.mil

ABSTRACT

This work demonstrates the dynamic control of light emission from a magnesium / polytetrafluoroethylene (Mg/PTFE) pyrotechnic through microwave irradiation (2.46 GHz, 1 kW CW). Pyrotechnic combustion experiments were conducted within a multimodal microwave cavity and were instrumented with UV-VIS spectroscopy, color video, and two-color high-speed video pyrometry. Microwave irradiation was found to increase UV-VIS light emission of a typical combustion event by 120%. Increases in the flame volume are also observed. This emission enhancement primarily occurs between ~350 to 400 nm and is due to microwave absorption by the transition enhancement of the diatomic species MgO and MgF. In contrast to prior studies on microwave irradiation of Mg/alkali nitrate flames, significant enhancement of continuum emission is also observed from Mg/PTFE as a result of temperature enhancement of the condensed phase flame species. To a lesser extent, atomic species emission is observed to increase due to electronic transition enhancement. Moreover, chromaticity of Mg/PTFE combustion show that a shift in color is possible utilizing microwave energy, due to enhancement of molecular and atomic emission. Temperature measurements using both two-color video pyrometry and gray body fitting consistently show microwave irradiation results in temperature increases of ~100-300 K. Energy deposition to the Mg/PTFE system is hypothesized to primarily occur from dielectric and eddy current loss to condensed phase species within the flame (magnesium fluorides and carbon), and temperature enhancement is limited by volatilization of these species. This work demonstrates the ability to tune Mg/PTFE pyrotechnic light emission output, more specifically enabling dynamic, on-command control of the light emission color and intensity.

INTRODUCTION

The light emission spectrum and color purity of pyrotechnics are of particular importance in the field of visible light-emitting pyrotechnics. Specifically, meeting dominant wavelength, color purity, and light-emission requirements are commonly achieved by tailoring the pyrotechnic composition through the addition of various colorant additives (e.g., perchlorate and nitrate salts, barium, sodium, or strontium).[1] Typically, pyrotechnics are formulated to achieve one of several goals, including signaling, illumination, or optical obscuration (e.g., through either strobe light emission or smoke production). The wide variety of applications met by pyrotechnics complicates manufacturing and implicates how a service person and/or aircraft/vehicle use the different pyrotechnics for various purposes. The optimization of light-emission properties through formulation and manufacturing can be laborious and, like solid propellants, offers no real-time method to control light emission brightness or color once a formulation is selected and pyrotechnic articles have been fabricated. Moreover, light-emission design through formulation is further constrained due to the environmental and toxicological hazards of some currently

utilized colorants and additives (e.g., perchlorates, heavy-metals, strontium additives, and barium additives, to name a few).[2] The development of pyrotechnics with dynamically tunable light-emission characteristics may solve some of the aforementioned pyrotechnic limitations while improving the color purity and light output of more environmentally friendly compositions.

Electric fields have been demonstrated as a way to dynamically modified and deposit energy into a flame in a number of different ways, which are summarized in Refs.[3,4] Briefly, static and low-frequency electric fields result in acceleration of electrons over long distances, that alter bulk transport effects within flames via ionic winds.[5–7] Higher frequency electric fields (e.g. MHz and higher frequencies) result in significant energy deposition to neutrals due to electron-neutral collisions when collision rates exceed the field frequency.[8] These collisions excite internal energy states of molecules (vibrational and electronic), as well as the production of additional radicals and ions through dissociation and ionization, ultimately resulting in electric field-supported plasma in the flame kernel. A number of plasma-assisted combustion studies have examined the ability of high-power radiofrequency or microwave fields to promote combustion in gas phase systems [9,10] Such plasmas can also activate new kinetic pathways and lead to important non-equilibrium energy distributions as energetic electrons efficiently transfer energy to vibrational modes and excited electronic states in the system.[11,12]

Electric field interactions with multiphase combustion systems has been demonstrated to have a number of different effects.[13–15] In previous work with aluminized solid composite propellants, microwave energy (2.46 GHz) deposition to the flame was shown to increase by adding small quantities (16 wt. %) of low-ionizing dopant, $NaNO_3$, and resulted in burning rate increases of up to 60%.[13] Moreover, in magnesium-based pyrotechnic systems containing high amounts of alkali nitrates, microwave fields have been demonstrated to increase visible emission up to 120% and able to sustain a plasma and light emission within pyrotechnic combustion products long after the extinction of combustion.[14,15] The addition of easily ionizing materials such as alkali nitrates are hypothesis to increase microwave deposition efficiency to flames due to increase electron/ion populations and are enough to support a microwave plasma. It should be noted that the coupling of electromagnetic fields with metalized multiphase flames such as those from pyrotechnics are complex.

In addition to the electron collisional effects observed in gas-phase flames, microwave energy deposition can occur in several other ways including (1) dielectric losses (dipolar polarization), (2) interfacial losses due to grain/phase boundaries and defect regions (Maxwell-Wagner polarization), and (3) conduction losses (eddy current or magnetic inductions heating). This is due to the nature of condense phase reactants/products existing in the flame. Dielectric heating of non-metalized condenses phase reactants is expected to be low due the microwave transparency of many ingredients.[16,17] Microwave loss in metal fuel reactants (particle sizes on the order of nm to μm) is expected to be higher due to eddy current heating,[18] which for spherical metals is a function of the particle size and microwave penetration depth.[19,20] A study on modelling microwave heating of metal particles coated with an oxide shell shows that electric field heating depends on the oxide shell properties (low conductivity), while magnetic field heating from eddy current generation is only dependent on the metal core properties.[21] Metal/metal oxide heating simulations at higher temperatures suggest magnetic field heating slows down once the Curie temperature is reached.[22] At elevated temperatures expected in the flame, dielectric heating of condense phase metallic oxides suffers from thermal runaway, in which dielectric absorption increases exponentially.[23] In aluminized solid composite propellant, microwave energy deposition to condensed-

phase metal oxide products within the propellant flame was observed and attributed to dielectric heating of high temperature metal oxides.[13,24]

In this work, the effects of microwave irradiation on the flame temperature of an Mg/PTFE pyrotechnic flame are explored. Small pyrotechnic articles are burned inside a 1 kW, 2.46 GHz multimode microwave cavity, where the electric field produces a plasma kernel in the combustion plume with unique spectral features. The effects of microwave field application on the light emission intensity, spectral features, and condensed-phase temperatures are investigated with UV-VIS spectroscopy and two-color video pyrometry to assess the ability to dynamically tune pyrotechnic flame temperatures with electric fields.

EXPERIMENTAL SECTION

Pyrotechnic Manufacture

The bimodal pyrotechnic formulation (Mg/PTFE, 1/1 wt. ratio) used in this study consisted of Mg fuel (Firefox; 190-325 mesh) and PTFE (Sigma Aldrich, 35 micrometer). The pyrotechnic composition was hand-mixed with a metal spatula within an electrically-grounded pan in quantities of less than 10 g. The fuel and oxidizer were mixed until homogeneous and brushed through a 100-mesh sieve. To achieve the desired consolidation density, reactive compositions were shim-pressed in a 6-mm diameter die to a nominal length of 9 mm using a Carver 12-ton press with a dwell time of approximately 10 seconds. Densities of the resulting pellets were approximately 98% TMD (theoretical mass density). Pellets were inhibited with an acrylic lacquer to prevent flame spread down the sides of the pellet.

Equilibrium Chemical Calculation

With higher fuel content pyrotechnic formulations, air diffusion will occur. To gain insight on microwave field deposition of flame products, electron concentrations, and flame temperature, chemical equilibrium calculations were conducted using the NASA Chemical Equilibrium with Applications (CEA) code using the enthalpy-pressure combustion module (hp) at a constant pressure in anaerobic atmospheric conditions (1 atm), where air was swept over a range of values.[25] In these calculations, the assumed heat of formation of the PTFE (C_2F_4) was -810 kJ mol^{-1}. Calculations were conducted with ionic chemistry enabled.

Microwave Combustion Cavity

A continuous, multimode microwave cavity (Figure 1) connected to an ~2.46 GHz magnetron (Galanz, M24FC-610A, 1.1 kW output) powered by a continuous high voltage power source (Glassman High Voltage Inc., LT5R400, 1.8 kW output) was used for experiments. The pyrotechnic was placed in an electric-field (E-field) antinode on a microwave-transparent PTFE block. The location of the field antinode was determined both experimentally and analytically. Experimentally, the E-field antinode location was found by imaging a liquid crystal film placed at various locations within the unloaded cavity during microwave irradiation. The experimentally determined location of the E-field antinode was consistent with simulations of the field distribution within the cavity that were conducted with COMSOL Multiphysics 5.0 (Fig. 1c). Based on separate experimental measurements of the field strength conducted with the same cavity and magnetron operated in a 60 Hz modulated mode,[15] we estimate the average RMS field strength for these experiments to be 2.7 kV/m.

The top surface of the pyrotechnic article was ignited with a continuous-wave diode laser (3.0 s illumination, 5 W, 450 nm). The combustion of pyrotechnic samples was monitored by a two-color pyrometer (20 Hz) and a UV-VIS spectrometer configured with a narrow collection angle to sample emission near the burning surface. The collection systems are indicated in Figure 1a. Direct emission from the near-burning-surface flame region was obtained by imaging light emission onto a 1000-µm multimode optical fiber (Thorlabs M35L01, 0.39 NA) optical fiber and into a separate spectrometer (OceanOptics HR4000, 10-Hz rate). Based upon positioning and the acceptance angle of the fiber, the sample collection volume is estimated to be a 5 cm diameter region centered 1.5 cm above the unburned pellet surface. The system response of spectrometer was spectrally corrected using a UV-VIS calibration source (OceanOptics DH-2000-CAL). Volumetric gray body temperature measurements of spectra were calculated using a MATLAB program, where continuum emission (500-850 nm, with no atomic or molecular features) was fitted using a similar procedure to Ref.[26] Emissivity calculated from the spectral fits are not real values due to the relative intensity calibration of the spectrometer (i.e. solid angle is unknown). Moreover, time integrated emission spectra and total emission intensity were calculated from spectrometer measurements during the entire burn. All instruments were triggered using a digital delay generator (Berkeley Nucleonics, Model 575). Color video of the flame event was acquired using a Phantom v9.0 with a zoom lens at exposure time of 4 µs and at frame rate of 200 Hz. Color video was not acquired at the same time as the other diagnostics.

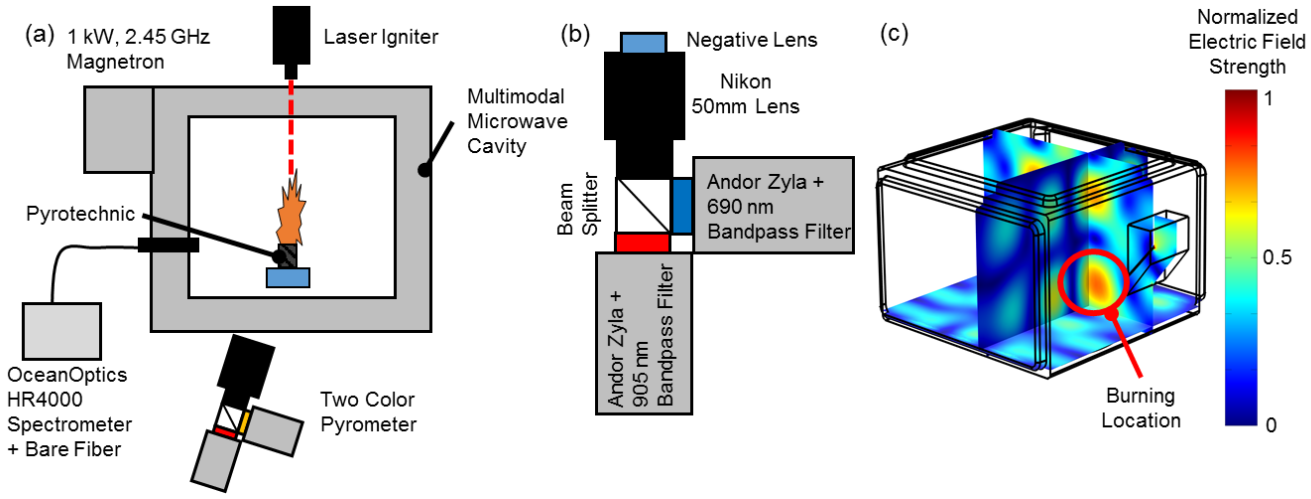

Figure 1. (a) Schematic of the microwave multimodal cavity with optical diagnostics including a two-color pyrometer, and two fiber-coupled spectrometers. (b) Schematic of two-color pyrometer, which includes a negative lens, a 50 mm Nikon compound lens, a 50/50 beam splitter, bandpass filters, and cameras. (c) COMSOL 5.0 simulation of normalized electric field distribution within the multimodal cavity. The red circle indicates burning location, which is located at an E-Field antinode.

Two-Color Video Pyrometry

Due to the high degree of condensed phase products within Mg/PTFE flames, a significant portion of light emitted is from gray body emission of soot, magnesium oxide, and magnesium fluoride.[27,28] As such, a reasonable estimate of the flame temperature may be made from gray body emission radiometric techniques. Previous work on flame temperature measurements of Mg/PTFE (33/67 wt.%) loose powder beds ignited in air has been determined from gray body fitting of near-infrared continuum emission,

where time-averaged Mg/PTFE temperatures were 2020 K, which is substantially lower than CEA predicted adiabatic temperature of ~2690 K.[28] Flame temperatures of Mg/PTFE pyrotechnics with Viton fluorocarbon binders have been studied as well. Near-IR spectra of rich Mg/PTFE/Viton (57/33/10 wt.%) pyrotechnic pellet combustion in air fitted with a gray body spectrum was reported with temperatures ranging from 1900 K to 2250 K.[29] However, Mg/PTFE combustion flame temperature has not been studied on spatial scale. By selecting two wavelength bands with relatively high gray body continuum signal, while avoiding molecular or atomic band emission, video pyrometry can be used to spatially and temporally resolve temperatures of the condensed phase products of the flame.[30–32]

Two Andor Zyla 5.5 sCMOS monochrome cameras (12-bit depth, 5.5 megapixels, 20 Hz, 9 µs exposure) were utilized for two-color video pyrometry of the pyrotechnic flames. The pyrometer imaged the combustion event through a Faraday cage screen. Briefly, light entered a negative lens (Thorlabs, 25 mm Ø, N-BK7 plano-concave lens, -75 mm focal length) and then through a Nikon 50 mm primary macro lens (.11 magnification, ~2 cm depth of field). The image was then split using a non-polarizing beam splitter (Figure 1b), were each path includes a bandpass filter (690 nm ± 10 nm FWHM, Thorlabs FB690-10; 905 nm ± 10 nm FWHM, Thorlabs FL905-10, respectively) prior to incidence on the detectors. The bandpass filters were selected based on analysis of emission spectra in order to verify the absence of molecular/atomic emission spectral features at these two wavelengths. More details about calibration and setup can be found in Ref.[24]

RESULTS AND DISCUSSION

Mg/PTFE combustion was studied with and without microwave enhancement using several different diagnostics, in which flame temperatures, flame structure, and UV-VIS emission was measured. Distinct changes in Mg/PTFE light emission were observed in all diagnostics as a result of microwave deposition to the pyrotechnic flame.

Chemical Equilibrium Calculations

Chemical equilibrium calculations were conducted on a 1:1 mass ratio of Mg/PTFE to gain insight on the effects of air addition (0 wt. % to 80 wt. % air). Figure 2 shows a diagram of a fuel-rich pyrotechnic flame products and the predicted adiabatic flame temperature and major equilibrium products of fuel-rich Mg/PTFE combustion (1:1 wt. ratio) with the addition of air from 0 to 80 wt. %. For anaerobic combustion, the predicted adiabatic flame temperature is 2360 K. Anaerobic combustion equilibrium products include a significant quantity of condensed-phase products (25.5 wt. % of total products) predominantly consisting of $MgF_{2(l)}$ and $C_{(gr)}$. Anaerobic conditions were hypothesized to be more representative of the flame's inner core.

Air addition to the fuel-rich Mg/PTFE composition has several effects on equilibrium products that are relevant to the pyrotechnic tested. With the addition of excess air (up to 41 wt. %), carbon products ($C_{(gr)}$) is reduced due to the formation of CO, as shown in Figure 2b. Further air addition beyond ~41 wt. % leads to oxygen reacting with excess Mg fuel to form $MgO_{(cr)}$ and $MgO_{(g)}$. Though air species advection into the flame is not known, it was expected that similar compositional effects would occur radially in the combustion of the fuel-rich Mg/PTFE pyrotechnic in air. Secondary reaction of air and premixed Mg/PTFE combustion products is expected and will result in the oxidization of excess Mg and carbon products and additional heat release. At an air fraction beyond ~44 wt. %, flame temperatures exceeded the volatilization temperature of $MgF2_{(l)}$ to form additional $MgF_{(g)}$ and $MgF2_{(g)}$. A maximum flame

temperature of 2920 K occurred with 60 wt. % air addition. Near this composition and temperature, equilibrium calculations predict maximum ionization (MgF^+ and Mg^+) and free-electron concentration (maximum of 8×10-4 product mol. fraction). Comparing these CEA results with Mg/alkali nitrate pyrotechnics (0.03-0.17 product mol. fraction), electron populations of the Mg/PTFE flame were orders of magnitude less.[15] Moreover, gas-phase flame neutral species are predominantly diatomic molecules, wherein Mg/alkali nitrate pyrotechnics, most of the gas-phase products are from neutral alkali atomic and Mg atoms. As a result of this, a majority of emission enhancement was of the alkali metal transition, and little molecular emission was observed.

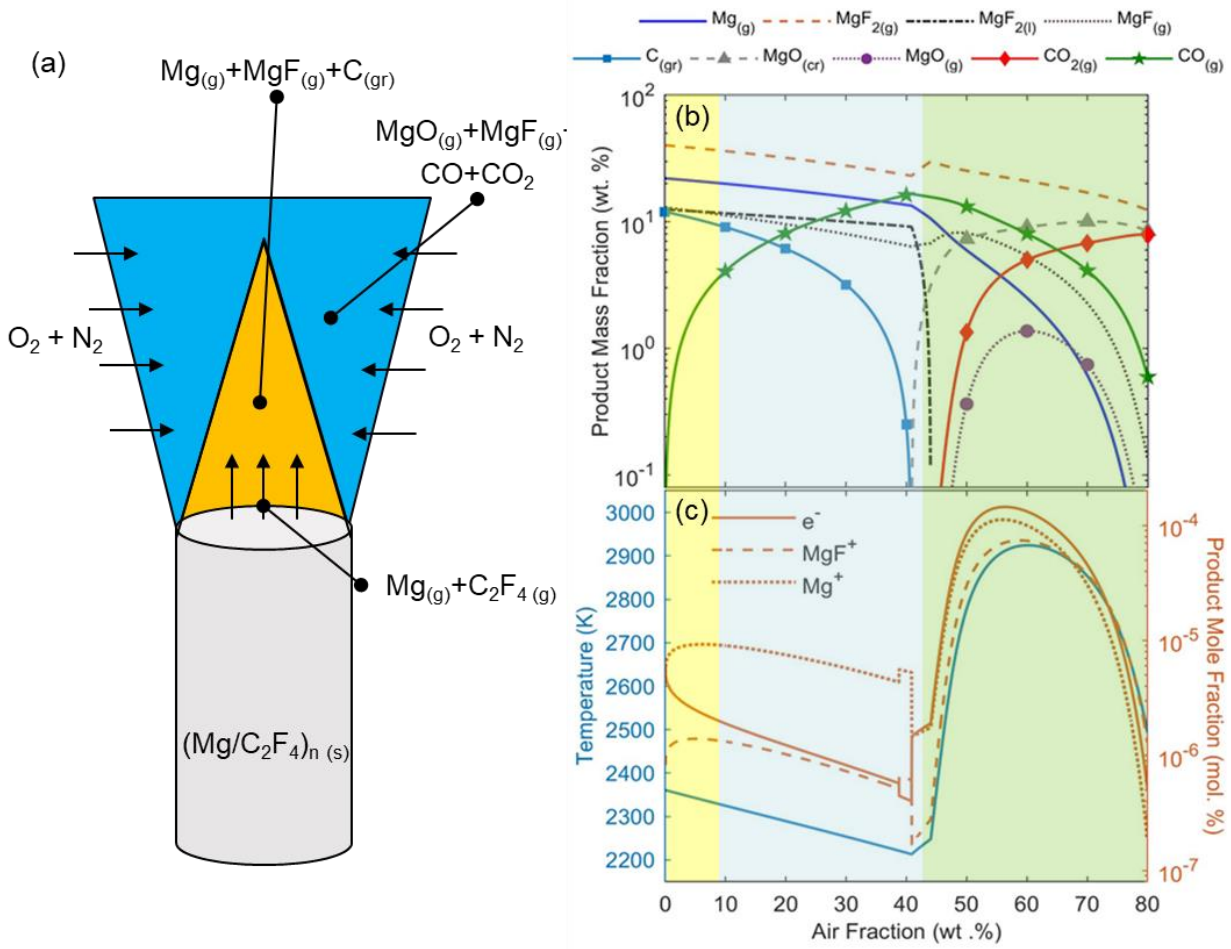

Figure 2. (a) Diagram of fuel rich Mg/PTFE flame products with air diffusion. (b) Equilibrium product mass fraction and (c) adiabatic flame temperature and most prevalent ion/electron mole fractions calculated as a function of air fraction for fuel-rich Mg/PTFE combustion (50/50 wt.%) at 1 atm pressure.

From equilibrium calculations, we hypothesized that electric field interaction with the flame would be spatially dependent. At the radial extent of the flame and at high standoff distances, where air-entrainment is highest, the microwave field will deposit energy to free-electrons and subsequently into molecular/atomic transitions. This is due to the high equilibrium ion/electron concentrations and lower condensed-phase carbon that is predicted with high air fraction. In the interior of the flame and at low standoff distances, we hypothesized that dielectric energy deposition to the condensed-phase would be

more significant due to the prevalence of products such as carbon ($C_{(gr)}$) and oxides/fluorides of magnesium ($MgF_{2(l)}$ and $MgO_{(cr)}$).

Spectral Emission Enhancement

Figure 3 shows the typical spectral emission of Mg/PTFE combustion (no microwave, blue), in which time-integrated spectra from three trial burns were averaged. Typical emission features of Mg/PTFE combustion in the absence of the microwave field include low-signal band emission from molecular MgF/MgO UVA bands (350-390 nm) and MgO green bands (476-521 nm),[27] and weak atomic emission from Mg, Na, Li, and K; transitions are summarized in Table 1. Atomic band emission from Na, Li, and K were a result of contaminants in the reactants. The majority of the visible emission is from the gray body continuum, which is due to the presence of high temperature, high emissivity carbonaceous species, and metal oxide/fluoride condensed-phase products that occur in Mg/fluorocarbon flames.[27,33]

With microwave illumination, significant enhancement of molecular, atomic, and gray body continuum emission was observed (Figure 3a, red). The majority of microwave-induced emission enhancement occurs from molecular electronic transitions. The MgF/MgO/Mg UVA band emission is increased by a factor of 30. Microwave emission enhancement of the MgO green bands also occurs, and several other molecular spectral features that are not observable without microwave illumination were detected, including MgO red bands (470-690 nm). Enhancements of atomic emission from Mg, Na, Li, and K (aforementioned transitions) along with the UVB transition of Mg (285 nm) were also observed. As a result of the microwave field, an increase in gray body continuum emission results in an increase in the condensed-phase product temperature of ~130 K, as seen in the gray body continuum fits in Figure 3a. Finally, the time- and wavelength-integration of the UV/VIS/NIR Mg/PTFE flame emission during combustion (260 nm to 900 nm) shows that microwave illumination results in an increase in total emission output of 90% (Figure 3b).

Table 1: Summary of molecular and atomic electronic transition observed with and without (baseline) microwave illumination.

Species	Wavelength (nm)	Transition	No Microwave*	Microwave*
MgF	265-274	$B^2\Sigma^+$-$X^2\Sigma^+$	o	x
MgF	347-369	$A^2\Pi$- $X^2\Sigma^+$	x	x
MgO	367-382	$C^1\Sigma^-$ - $A^1\Pi$	x	x
MgO	470-690	$B^1\Sigma^+$-$A^1\Pi$	o	x
MgO	476-521	$B^1\Sigma^+$- $X^1\Sigma^+$	x	x
Mg	285 (Singlet)	3s3p-$3s^2$	o	x
Mg	383 (Triplet)	3s3d-3s3p	x	x
Mg	517 (Triplet)	3s4s-3s3p	x	x
Li	671 (Doublet)	2p-2s	x	x
Na	589 (Doublet)	3p-3s	x	x
K	767 (Doublet)	4p-4s	x	x

*x, detected; o, not observed.

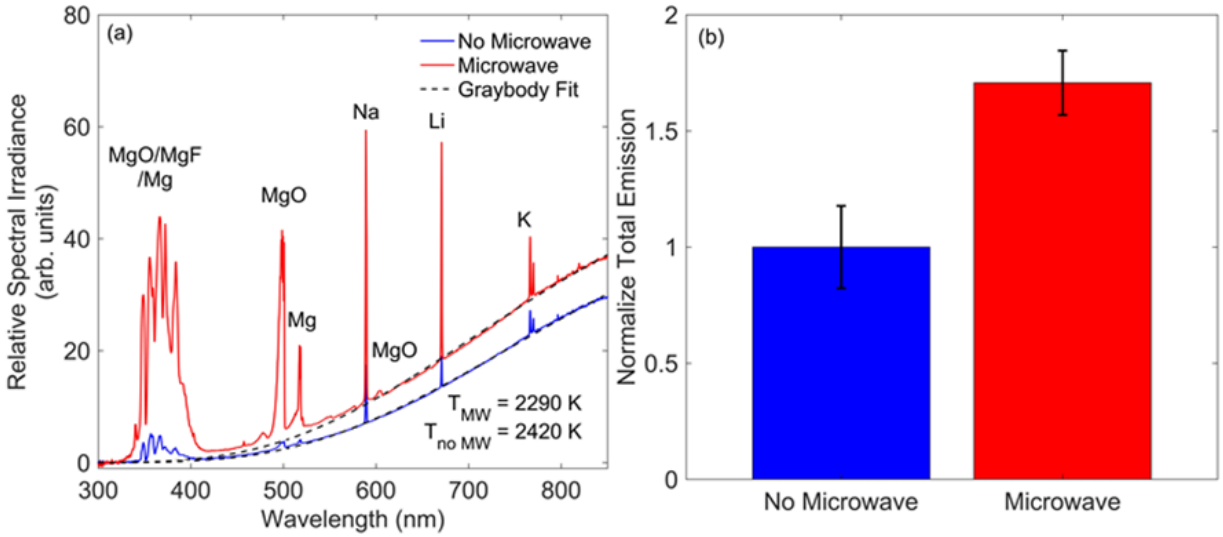

Figure 3. (a) Time-integrated UV-VIS emission spectra from Mg/PTFE combustion with and without microwave irradiation (averages of three trials each). Microwave irradiation increases emission from molecular bands (MgO and MgF), atomic bands. Gray body fits represent average temperatures from entire burn durations. (b) Normalized total irradiance of Mg/PTFE pyrotechnics with and without microwave illumination. Values and error bars represent the average and standard deviation of three trials, respectively.

Microwave Effects on Flame Structure

Image sequences of the Mg/PTFE flame are shown with and without microwave field application in Figure 4. Microwave irradiation of the flame results in an increase in both light emission intensity and a shift in dominant color. For Mg/PTFE pyrotechnic combustion without microwave irradiation, the flame structure and intensity appear uniform over the time duration of ~50 ms. The flame appears white/red with most of the visible emission resulting from the condensed-phase products. However, with microwave application, flame intensity, and emission volume increase significantly.

Flame emission features are observed farther away from the burning surface, and flame structure temporal instabilities are observed, as microwave energy continues to deposit energy into hot combustion products as it travels further away from the burning surface. Significant increase in blue emission, which surrounds the inner portion of the red/white flame. This inner portion of the flame is more likely to be a condensed-phase gray body emitter, in which emission from the condensed-phase height is greater than without microwave deposition. Moreover, the blue, outer flame is most likely due to enhancement of MgO/MgF band emission at 350-400 nm, MgO multiplet (490-520 nm), and Mg I (383.7 nm and 518.4 nm), which the Bayer filter is optimized for 400-500 nm for blue pixels. This enhancement of blue emission cannot be seen in the no microwave case.

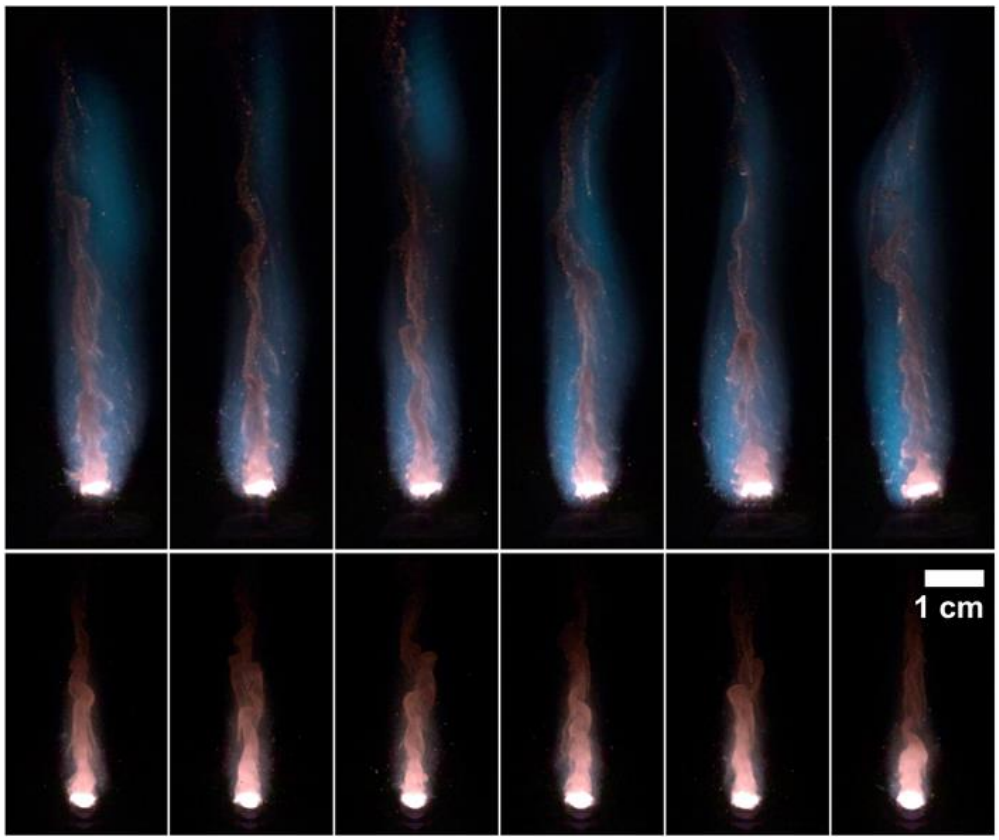

Figure 4. Color image sequences of Mg/PTFE combustion taken with (top) and without (bottom) microwave illumination. Image sequences are acquired with the same exposure settings (2 μs).

Chromaticity and Luminosity Effects

Microwave illumination of Mg/PTFE resulted in a highly time-dynamic shift in chromaticity that occurs from the excitation of visible atomic/molecular electronic transitions in the secondary air diffusion flame. The time-dynamic emission is more observable in images and supplemental videos acquired using higher exposure time (Figure 5a) and corresponding chromaticity calculations performed on emission spectra obtained during these periods (Figure 5b). Without the microwave field application, the gray body continuum dominates the visible light emission spectrum. This can be seen in Figure 5b, as flame chromaticity (green dots) follows the trend of a black body emitter (dotted line) on the diagram. With microwave illumination, the three-time periods—(I) pre-combustion, (II) combustion, and (III) post-combustion—are found to each have unique effects on flame chromaticity.

Prior to Mg/PTFE ignition, both the top ignition laser (450 nm, 3-second duration) and microwave source illuminated the pyrotechnic sample. During this period, a ~100 to 300 ms duration light emission event occurs in which a plasma kernel is formed at the burning surface and, with support of the microwave field, continues to emit as it advects upward. This region is indicated in the top image montage of Figure 5a. It was hypothesized that during pre-ignition, laser energy was absorbed in the top surface of the pellet, which caused the vaporization of magnesium and subsequent oxidation with air to produce MgO. From the microwave interaction with gas-phase, electron collisional excitation of MgO and Mg vapor species produced emission. This hypothesis is consistent with the emission spectra of the cyan plasma during the

pre-combustion event, which contains emission from MgO green bands. Chromaticity calculations of emission spectra (Figure 5) show that light emission during the pre-combustion period is cyan.

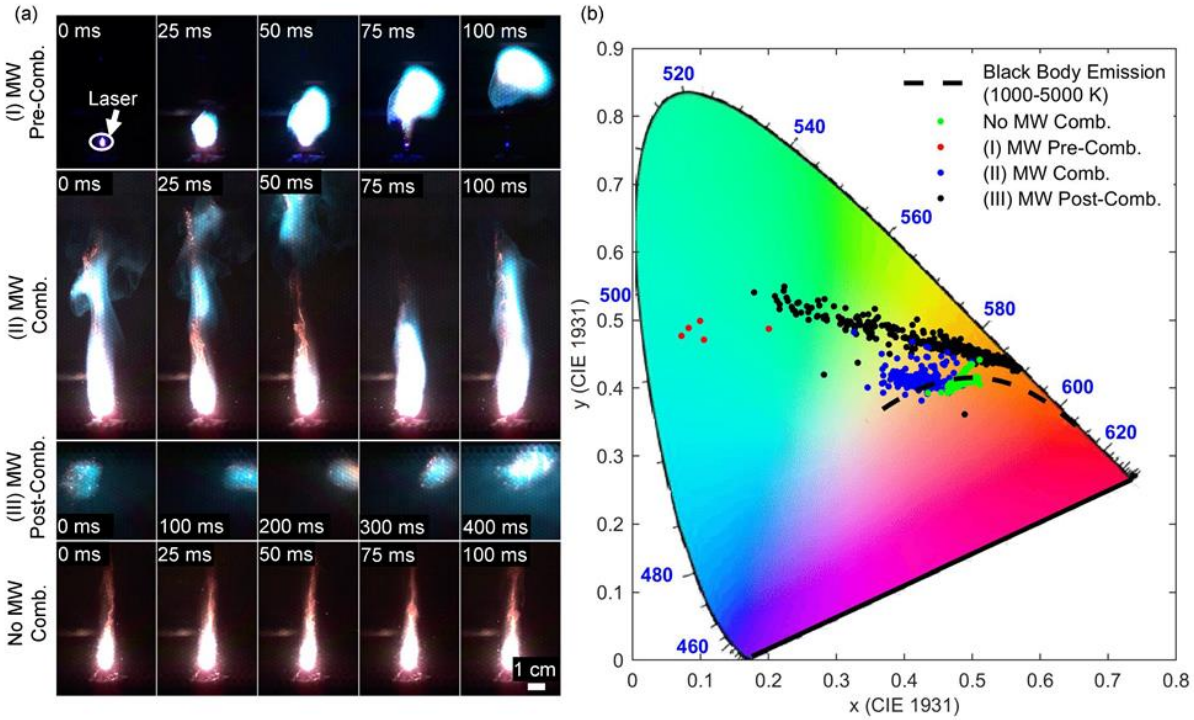

Figure 5. (a) Color image sequences of Mg/PTFE combustion taken with (top) and without microwave illumination. Image sequences are shown for the three different light emission regimes observed because of microwave illumination (I) pre-combustion, (II) combustion, and (III) post-combustion extinguishment light emission. Image sequences are acquired with the same exposure settings (200 Hz, 200 µs). (b) CIE 1931 chromaticity diagram showing time-resolved color and purity of emission from Mg/PTFE pyrotechnic.

During the normal combustion period, the chromaticity diagram shows (Figure 5) that microwave illumination shifts emission from an orange ~2200 K black body color (without microwave illumination) toward a whiter, less spectrally pure color due to both strong MgO green band emission and continuum emission. During this period, microwave illumination results in ~90% increase in illumination intensity (Figure 3b). Flame emission features are observed farther away from the burning surface, and temporal instabilities are observed as hot products advect from the surface and continue to couple with the microwave field.

After combustion extinguishment, microwave illumination results in continued light emission from a post-combustion plasm. Light emission extraction was possible for a duration of ~10 seconds, after which the microwave field was turned off, as seen in the spectra time history shown in Figure 6. Emission during the post-combustion period is of much lower light intensity (Figure 6c) and occurs primarily from atomic/molecular species. Time integrated emission is comprised of Na atomic emission (589 nm), MgO green and red emission bands (476-521 nm and 470-690 nm), and the UVA emission bands (350-400 nm).

With microwave illumination, MgO, Mg, and Na features cause a shift in post-combustion chromaticity, resulting in dominant colors of green, yellow, and orange.

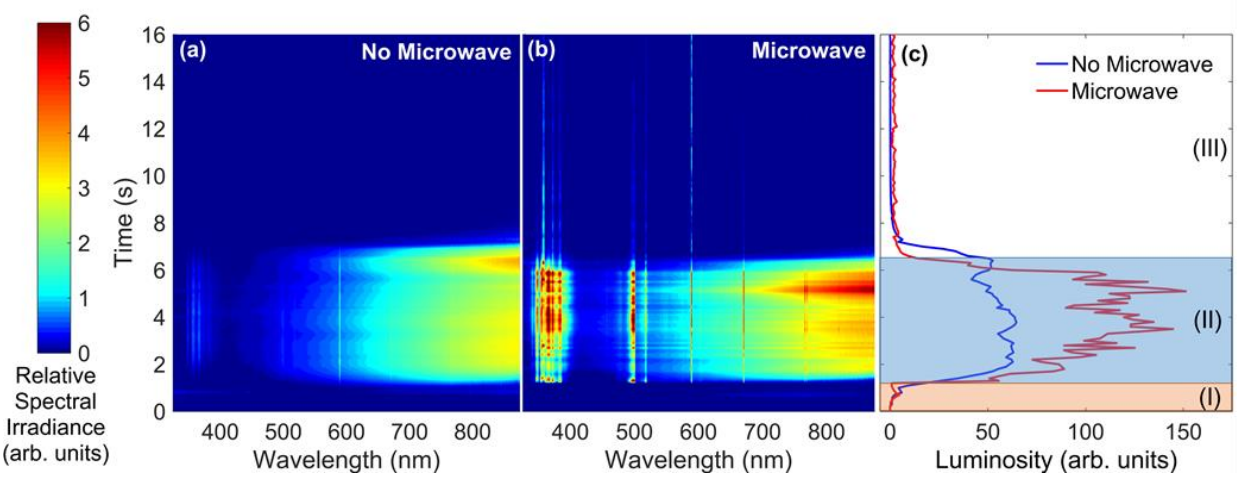

Figure 6. Typical spectra time histories of Mg/PTFE combustion both without (a) and with (b) microwave illumination. Panel (c) shows the wavelength-integrated total luminosity of the time series, where (I), (II), and (III) represent pre-combustion, combustion, and post-combustion, respectively. Pyrotechnic combustion starts at approximately 1 s and extinguishes at 7 s. Post-combustion emission occurs after 7 seconds with microwave illumination.

In comparison to the combustion of Mg/alkali nitrate pyrotechnics,[15] microwave illumination of Mg/PTFE flames resulted in a significant enhancement in the continuum and molecular emission features. Investigated previously, the quantity of alkali nitrate in formulations was high (49.4 to 66.5 wt.%), and the negligible continuum or molecular emission enhancement was observed under similar microwave field strengths.[15] Instead, the dominant emission feature was that of resonance-broadened Na D-line emission.[34] Consequently, the high alkali concentration of such flames results in preferential excitation and emission from atomic alkali neutrals. In this study, the color of flames from alkali nitrate-based pyrotechnics is not changed, and only luminous intensity is affected.

Flame Temperature Measurements

The temporal-resolved gray body temperatures of the pyrotechnic plume can be seen in Figure 7a, where spectra of the continuum are fitted using Planck's equation for the region between 500 to 850 nm, excluding discrete atomic and molecular emission features. For both the baseline (no microwave) and microwave-illuminated cases, a period of constant temperature (steady burning) and a subsequent drop in temperature corresponding to extinguishment are observed. Experiments without microwave had an average gray body flame temperature of 2300 K during steady burning. An increase in gray body temperature of approximately 100-300 K is observed as a result of microwave irradiation. These results are in contrast to a similar study of Mg/alkali nitrate pyrotechnic formulations,[15] where microwave irradiation resulted in almost no continuum emission enhancement. In alkali nitrate systems investigated previously, the quantity of alkali-nitrate in formulations was high (66.5, 52.2, and 49.4 wt. % of Cs, K, or Na nitrate, respectively). The high alkali concentration of such flames results in higher electron number densities, a relatively low concentration of condensed-phase species (estimated from adiabatic flame conditions), and as a result, preferential microwave energy deposition electronically to the alkali atomic species.

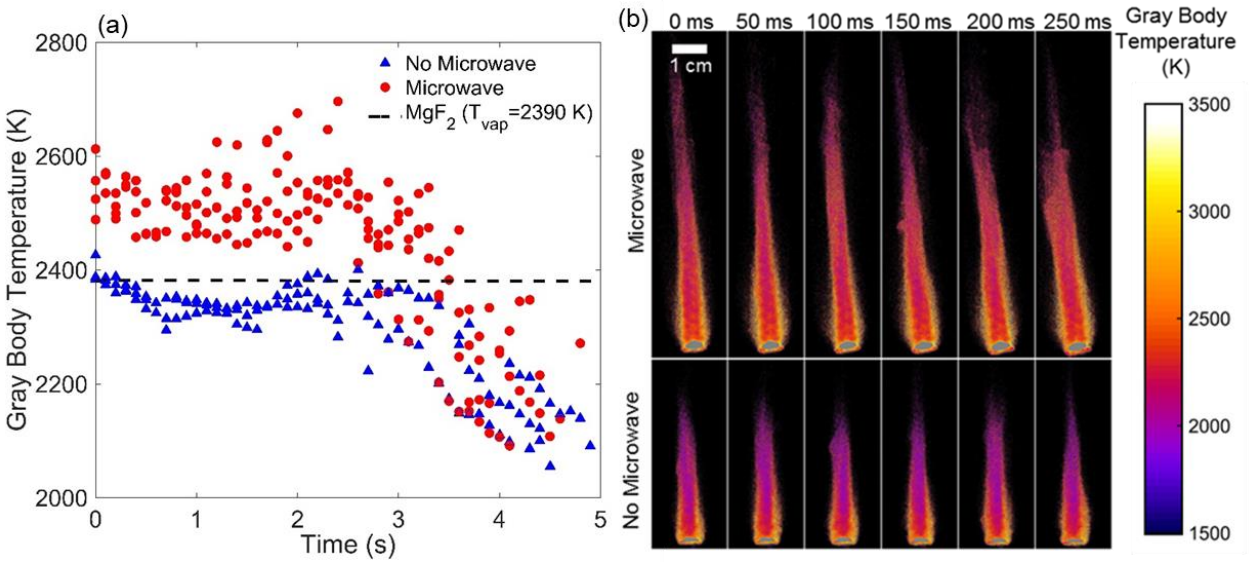

Figure 7. (a) Time-resolved gray body temperature fits of visible spectra taken from three experimental trials both with and without microwave irradiation. The boiling temperature of MgF_2 at 1 atm is indicated by a dashed line. (b) Temperature map image sequences of the Mg/PTFE flames with (top) and without (bottom) microwave irradiation. An increase in flame volume and temperature of the Mg/PTFE flame are observed. All measurements are taken using detector exposures of ~9 µs. Gray regions represent pixels in which one of the two pyrometer channels were saturated.

With two-color video pyrometer imaging of the pyrotechnic plume, a two-dimensional map of gray body flame temperature can be produced to investigate spatial effects. Images of flames without microwave application (Figure 7b, bottom) show flame temperatures in the range of 2000-2600 K occur during combustion, and flame structure is time-uniform throughout the sampling duration of 250 ms. The time-average temperature during the same 250 ms period of the entire flame with gray body signal is 2280 K, which is consistent with the aforementioned gray body temperatures measured for pyrotechnic combustion without microwave irradiation (Figure 7a). Moreover, this is consistent with aerobic equilibrium calculations reported elsewhere.[35] Further processing of the pyrometer temperature maps shows additional quantitative differences in Mg/PTFE pyrotechnic flame structure.

Figure 8a shows average flame temperature as a function of height from the burning surface. These temperatures (dark blue: no microwave and red data: microwave) represent spatially averaged temperature profiles collected from 0.5 s of steady combustion (approximately 10 single-shot image pairs from the pyrometer). Time-averaged radial temperature profiles (teal: no microwave and black data: microwave) at heights of 0.5 to 1.5 and 2.5 to 3.5 cm from the burning surface are also shown (Figure 8, respectively). The time-averaged radial temperature profile at a nominal height of 1 cm from the pyrotechnic surface (Figure 8b) clearly shows both premixed and diffusion flame structures both with and without microwave irradiation. For the premix region of the flame, combustion is expected to be mainly the Mg/PTFE reaction, while the diffusion flame occurs when oxygen diffuses inward into the flame, where it reacts with the fuel-rich premixed flame. For the case without microwave irradiation, the fuel-rich flame is comprised of a premixed flame zone within the core of the flame (~2100 K) that is surrounded by a hotter diffusion flame zone (~2500 K).

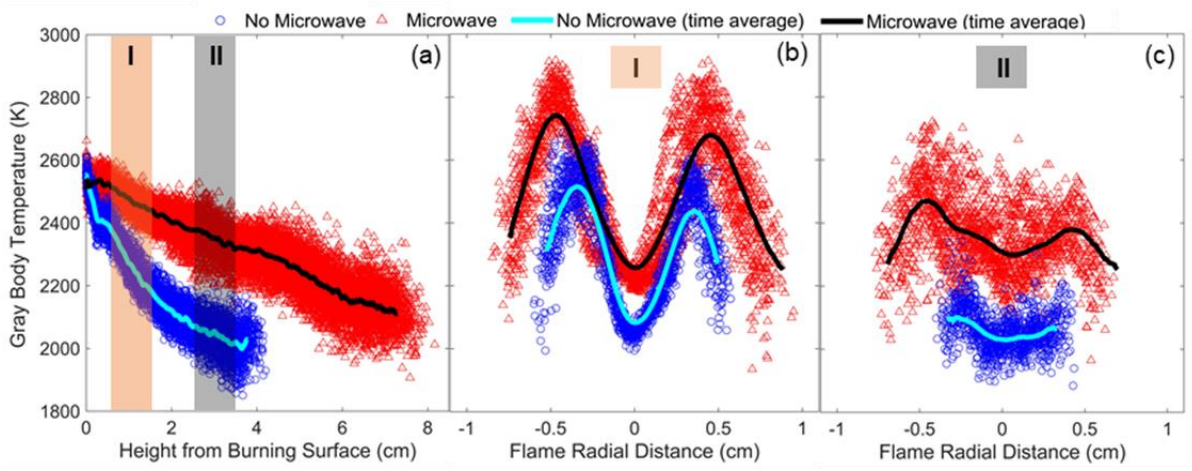

Figure 8. (a) Pyrometer average temperature profile as a function of height from the burning surface. Shaded areas I and II represent height ranges above the burning surface from which radial temperature profiles (b,c) are calculated. (b) Radial average temperature profile cross-sections of the flame are shown at heights above the burning surface of 0.5 to 1.5 cm (b) and 2.5 to 3.5 cm (c). All plots comprise temperature measurements from approximately 10 pyrometer images spanning a 0.5 s duration during the steady combustion period of one pyrotechnic burn. The time-averaged plots utilized smoothing to reduce noise.

With the application of microwave irradiation to the pyrotechnic flame, the flame volume and condensed-phase temperatures are enhanced (Figure 7b, top). The vertical height of the pyrotechnic flame (Figure 8a) is approximately doubled from 4 cm to 8 cm, while the flame diameter increases from 1 cm to 1.5 cm (Figure 8b). Moreover, increases in both the premixed (~2250 K) and diffusion flame zone temperatures (~2750 K) are observed, suggesting an increase in condensed-phase product temperatures due to microwave irradiation. The premixed flame temperatures increase by ~150 K, where the center of the flame represents the premixed region. The diffusion flame is higher in temperature than the premixed flame region and exhibits a larger temperature increase of ~200 K under microwave irradiation. The time-averaged temperature of the flame volume is 2400 K, which is a total increase in temperature of 130 K with microwave deposition to the flame.

Microwave Light Emission Enhancement Mechanism

Energy transfer to the primary (premixed) flame, secondary (air entrainment) flame, and to the condensed-phase reactants occurs primarily by three different mechanisms. The interaction of microwave fields with the primary flame of Mg/PTFE produces a significant enhancement of continuum light emission. A similar effect was observed as a result of microwave illumination of sodium-nitrate doped aluminized composite solid propellant flames.[13] The dielectric thermal runaway of aluminum oxide—exponential temperature dependence of dielectric loss [36]—was proposed as the mechanism for continuum emission enhancement in aluminized propellant products.

In the present work, anaerobic equilibrium calculations suggest the primary flame produces the condensed-phase product species $MgF_{2(l)}$ and carbon. MgF_2 exists in the liquid phase at anaerobic combustion temperatures ($T_{adiabatic}$, anaerobic = 2360 K), which is just below the MgF_2 volatilization temperature (T_{boil}= 2533 K). While dielectric thermal runaway is commonly observed in ceramics, the dielectric loss and dielectric temperature sensitivity of MgF_2 at high temperature are unknown.

Regardless, the potential for dielectric microwave heating of the MgF_2 condensed-phase is limited due to the adiabatic flame temperature being in close thermal proximity to the MgF2 volatilization temperature. Conversely, carbon microwave absorption is known to be high [37] and has a high sublimation temperature ($T_{sublimation}$ = 3915 K). Due to the anaerobic conditions of the primary flame, carbon is stable and expected to efficiently absorb microwave energy. Therefore, it was expected that observed continuum enhancement and measured flame temperature increase of ~150 K from microwave illumination was a result of dielectric heating of carbon condensed-phase products.

Together, equilibrium calculations, emission spectra, and color images suggest that one of the modes of microwave energy absorption in the secondary flame is electronic and results in excitation of molecular and atomic electron transitions. Electronic microwave absorption within the secondary flame occurs in part due to a lower concentration of dielectric absorbing carbon species. While lower condensed-phase was observed in the color images, an increase in condensed-phase temperature of 200 K is observed. This is expected to be a result of direct radiation/gas-phase heating of carbon, which is located in the enhanced blue emission secondary flame region. While the secondary flame is expected to contain $MgO_{(cr)}$, its dielectric microwave absorptivity is low. Microwave sintering experiments conducted on MgO by others [38] between 1400 and 1500 °C indicate that high-temperature MgO has low microwave loss that is insensitive to temperature. This is consistent with prior experiments on microwave enhancement of light emission from magnesium and alkali nitrate pyrotechnics where, despite the abundance of MgO combustion products (28-46 wt. %), negligible emission enhancement was observed.

From equilibrium calculations, higher air addition resulted in: (1) reduced carbon condensed-phase products, (2) higher flame temperatures, and (3) higher ion (MgF^+ and Mg^+) and electron populations. As such, it is expected that conditions within the secondary flame, where air-entrainment is expected to produce higher free-electron concentrations, are more favorable for electronic energy absorption. When exposed to a microwave field, the secondary flame region results in a higher ratio of the electric field to number density. Thus, higher rates of electron production and inelastic electron-neutral collisions lead to excited-state populations of atoms/molecules and subsequent photoemission. This effect is observable in images of the secondary flame (Figure 4) as blue emission and in spectra (Figure 3) as emission features from atomic (Mg) and molecular (MgO and MgF) neutrals.

Microwave heating of the condensed-phase pyrotechnic reactants may also occur and increase light emission intensity. While PTFE reactants are low dielectric loss materials even at elevated temperatures,[39] magnesium can be heated via eddy current [18] because the particle sizes are on the order of microwave penetration depth (orders of nm to μm).[19,20] Microwave heating of condensed-phase reactants could increase instantaneous luminosity through an enhanced burning rate. However, microwave heating of condensed-phase magnesium is expected to be small, as separate efforts on microwave sintering of Mg indicate heating rates are ~17 K/min (1 kW microwave field), which is lower than microwave heating rates of many other metals.[40] The dominant microwave absorption mechanism within the three combustion wave regions (primary flame, secondary flame, and reactants) are summarized in Table 2.

Table 2. Summary of microwave absorption and microwave-enhanced light emission characteristics of Mg/PTFE combustion wave regions.

Combustion Wave Region	Dominant MW Absorption Mode	MW Absorption Species	Characteristic Light Emission Enhancement	Light Emission Species
Primary Flame	Dielectric	$C_{(s)}$	Continuum (spectral, red)	$C_{(s)}$
Secondary Flame (air entrainment)	Electronic	e^-, forming MgF^+, Mg^+	Spectral, UVA/blue/green	$MgO_{(g)}$, $MgF_{(g)}$, $Mg_{(g)}$
Reactants	Eddy current	$Mg_{(s)}$	Uniform luminosity enhancement	N/A

CONCLUSIONS

This effort explored the ability to enhance the combustion of Mg/PTFE pyrotechnics utilizing a microwave field to deposit energy into the flame and dynamically control emission color and light intensity. Results indicated that microwave illumination increases UV/VIS/NIR light emission by ~90%. Microwave enhanced light emission includes both enhanced gray body and molecular/atomic electronic emission. Flame volume is shown to increase with microwave illumination, where both condensed-phase and gas-phase emission extend further away from the burning surface. A shift in emission color can be seen in both a chromaticity diagram and color imaging, in which cyan emission from both UVA I bands (MgO, MgF, and Mg I) and MgO green bands are mainly responsible for the shift. This enhanced cyan emission is consistent with microwave coupling to the predominantly gas-phase products of the high-temperature secondary diffusion flame formed from air entrainment with pyrotechnic combustion products. Equilibrium calculations suggest that within the secondary flame region, there is also a decrease in condensed carbon products and an increase in gas-phase MgO and MgF relative to the premixed flame region. Emission spectra showed an increase in gray body temperature of flames by approximately 100-200 K utilizing microwave irradiation to a flame, which was consistent with two-color pyrometer measurements. Equilibrium calculations on anaerobic Mg/PTFE combustion showed that adiabatic flame temperatures were thermodynamically limited by the vaporization of $MgF2_{(l)}$ with the formulation tested. Microwave deposition to a flame may be a way to reduce condensed-phase products in the flame and overcome this thermodynamic limit. Two-color video pyrometry was used to obtain spatially resolved temperature profiles within the flame. These results illustrate the effects of microwave irradiation on flame temperature and structure. Measurements showed microwave irradiation increases the temperature of the premixed flame core by ~150 K and the exterior diffusion flame sheet by ~200 K, respectively. Moreover, microwave irradiation results in a significant increase in the flame volume, both radially and axially.

This emission enhancement is hypothesized to be the combined result of (1) increased frequency of electron-neutral collisions resulting in increased electronic emission from gas-phase atomic and molecular species; (2) dielectric/eddy current heating by the condensed-phase combustion species (carbon); and (3) direct energy absorption of the condensed-phase reactants via eddy current heating. These results generally show the potential for dynamic color-shifting of pyrotechnic flames by non-

resonant excitation of exited electronic and molecular states via a microwave field. Additional characterization of the thermalization of the microwave field energy in the diffusion and premixed flame structure may provide insight into energy exchange pathways, which may be targeted to maximize color shift and luminous effects with applied fields. Specifically, light emission enhancement observed in both the primary and secondary flame zones suggests strategies to eliminate high dielectric loss condensed-phase combustion products from the primary flame combustion products may reduce gray body continuum light emission enhancement and enable higher color purity microwave enhanced luminosity.

ACKNOWLEDGMENTS

The authors wish to acknowledge financial support from the Strategic Environmental Research Development Program the direction of Dr. Robin Nissan. SJB wishes to acknowledge additional financial support from the Iowa State University Alliance for Graduate Education and the Professoriate program and the NASA Iowa Space Grant Consortium (NASA Award No. NNX16AL88H). NSWC Crane acknowledges financial support from Naval Innovative Science and Engineering Program.

REFERENCES

(1) Meyerriecks, W.; Kosanke, K. L. Color Values and Spectra of the Principal Emitters in Colored Flames. *J. Pyrotech.* **2003**, *18*, 1–22.

(2) Sabatini, J. J.; Nagori, A. V.; Chen, G.; Chu, P.; Damavarapu, R.; Klapötke, T. M. High-Nitrogen-Based Pyrotechnics: Longer- and Brighter-Burning, Perchlorate-Free, Red-Light Illuminants for Military and Civilian Applications. *Chem. - A Eur. J.* **2012**, *18* (2), 628–631.

(3) Ju, Y.; Sun, W. Plasma Assisted Combustion: Dynamics and Chemistry. *Prog. Energy Combust. Sci.* **2015**, *48*, 21–83.

(4) Starikovskiy, A. Physics and Chemistry of Plasma-Assisted Combustion. *Philos. Trans. R. Soc. London A Math. Phys. Eng. Sci.* **2015**, *373* (2048), 1–8.

(5) Lawton, J.; Weinberg, F. J. Maximum Ion Currents from Flames and the Maximum Practical Effects of Applied Electric Fields. *Proc. R. Soc. A Math. Phys. Eng. Sci.* **1964**, *277* (1371), 468–497.

(6) Marcum, S. D.; Ganguly, B. N. Electric-Field-Induced Flame Speed Modification. *Combust. Flame* **2005**, *143* (1–2), 27–36.

(7) Engineering, C.; Technology, C. Electrical Control of Solid Propellant Burning. *R. Soc.* **1964**, *284* (1399), 488.

(8) Ward, M. A. V; Wu, T. T. A Theoretical Study of the Microwave Heating of a Cylindrical Shell, Flame-Front Electron Plasma in an Internal Combustion Engine. *Combust. Flame* **1978**, *32*, 57–71.

(9) Michael, J. B.; Chng, T. L.; Miles, R. B. Sustained Propagation of Ultra-Lean Methane/Air Flames with Pulsed Microwave Energy Deposition. *Combust. Flame* **2013**, *160* (4), 796–807.

(10) Stockman, E. S.; Zaidi, S. H.; Miles, R. B.; Carter, C. D.; Ryan, M. D. Measurements of Combustion Properties in a Microwave Enhanced Flame. *Combust. Flame* **2009**, *156* (7), 1453–1461.

(11) Ombrello, T.; Ju, Y. Kinetic Ignition Enhancement of H2 Versus Fuel-Blended Air Diffusion Flames Using Nonequilibrium Plasma. *IEEE Trans. Plasma Sci.* **2008**, *36* (6), 2924.

(12) Mintoussov, E.; Pancheshnyi, S.; Starikovskii, A. Propane-Air Flame Control by Non-Equilibrium Low-Temperature Pulsed Nanosecond Barrier Discharge. In *42nd AIAA Aerospace Sciences Meeting and Exhibit*; Reno, 2004.

(13) Barkley, S. J.; Zhu, K.; Lynch, J. E.; Michael, J. B.; Sippel, T. R. Microwave Plasma Enhancement of Multiphase Flames : On-Demand Control of Solid Propellant Burning Rate. *Combust. Flame* **2019**, *199*, 14–23.

(14) Miklaszewski, E. J.; Dilger, J. M.; Crespo, W. F.; Michael, J. B.; Barkley, S. J. Electromagnetic Augmentation of Pyrotechnic Emissions. In *The 43rd International Pyrotechnics Society Seminar*; Fort Collins, 2018.

(15) Barkley, S. J.; Lynch, J. E.; Miklaszewski, E. J.; Dilger, J. M.; Crespo, W. F.; Michael, J. B.; Subramaniam, S.; Sippel, T. R. Microwave-Assisted Modulation of Light Emission Intensity in Alkali-Pyrotechnic Plumes. *Combust. Flame* **2021**, *225*, 406–416.

(16) Hasue, K.; Tanabe, M.; Watanabe, N.; Nakahara, S.; Okada, F. Initiation of Some Energetic Materials by Microwave Heating. *Propellants, Explos. Pyrotech.* **1990**, *15* (5), 181.

(17) Higginbotham Duque, A. L.; Lee Perry, W.; Anderson-Cook, C. M. Complex Microwave Permittivity of Secondary High Explosives. *Propellants, Explos. Pyrotech.* **2014**, *39* (2), 275–283.

(18) Gupta, M.; Eugene, W. W. L. *Microwaves and Metals*; John Wiley & Sons, Ltd: Singapore, 2011.

(19) Rybakov, K. I.; Olevsky, E. A.; Krikun, E. V. Microwave Sintering: Fundamentals and Modeling. *J. Am. Ceram. Soc.* **2013**, *96* (4), 1003–1020.

(20) Crane, C. A.; Pantoya, M. L.; Weeks, B. L.; Saed, M. The Effects of Particle Size on Microwave Heating of Metal and Metal Oxide Powders. *Powder Technol.* **2014**, *256*, 113–117.

(21) Biswas, P.; Mulholland, G. W.; Rehwoldt, M. C.; Kline, D. J.; Zachariah, M. R. Microwave Absorption by Small Dielectric and Semi-Conductor Coated Metal Particles. *J. Quant. Spectrosc. Radiat. Transf.* **2020**, *247* (106938), 1–8.

(22) Meir, Y.; Jerby, E. Thermite Powder Ignition by Localized Microwaves. *Combust. Flame* **2012**, *159* (7), 2474–2479.

(23) Sutton, W. H. Microwave Processing of Ceramic Materials. *Am. Ceram. Soc. Bull.* **1989**, *68* (2), 376.

(24) Zhu, K.; Barkley, S. J.; Sippel, T. R.; Michael, J. B. Flame Temperature Measurement of Microwave-Assisted Aluminum Particle Combustion. In *AiAA SciTech 2019 Forum*; San Diego, 2019; pp 1–10.

(25) McBride, B. J.; Gordon, S. NASA Chemical Equilibrium with Applications. NASA 2008.

(26) Terry, B. C.; Lin, Y. C.; Manukyan, K. V.; Mukasyan, A. S.; Son, S. F.; Groven, L. J. The Effect of Silicon Powder Characteristics on the Combustion of Silicon/Teflon/Viton Nanoenergetics. *Propellants, Explos. Pyrotech.* **2014**, *39* (3), 337–347.

(27) Koch, E. C. *Metal Fluorocarbon Based Energetic Materials*; Wiley-VCH: Weinheim, 2012.

(28) Koch, E. C.; Hahma, A.; Klapötke, T. M.; Radies, H. Metal - Fluorocarbon Pyrolants: XI. Radiometric Performance of Pyrolants Based on Magnesium, Perfluorinated Tetrazolates, and Viton A. *Propellants, Explos. Pyrotech.* **2010**, *35* (3), 248–253.

(29) Weiser, V.; Roth, E.; Muller, D.; Koch, E.-C. Investigation of Magensium-Fluorohydrocarbon-Flames Using Emission Spectroscopy. In *International Annual Conference of ICT*; Karlsruhe, 2006; Vol. 37th.

(30) Chen, Y.; Guildenbecher, D. R.; Hoffmeister, K. N. G.; Cooper, M. A.; Stauffacher, H. L.; Oliver, M. S.; Washburn, E. B. Study of Aluminum Particle Combustion in Solid Propellant Plumes Using Digital In-Line Holography and Imaging Pyrometry. *Combust. Flame* **2017**, *182*, 225–237.

(31) Mcnesby, K. L.; Homan, B. E.; Benjamin, R. A.; Boyle, V. M.; Densmore, J. M.; Biss, M. M. Invited Article : Quantitative Imaging of Explosions with High-Speed Cameras. *Rev. Sci. Instrum.* **2016**, *87* (051301), 1–14.

(32) Densmore, J. M.; Homan, B. E.; Biss, M. M.; McNesby, K. L. High-Speed Two-Camera Imaging Pyrometer for Mapping Fireball Temperatures. *Appl. Opt.* **2011**, *50* (33), 6267.

(33) Koch, E.; Weiser, V.; Roth, E.; Müller, D. UV-VIS Spectroscopic Investigation of Magnesium / Fluorocarbon Pyrolants. In *33rd International Pyrotechnics Seminar*; Fort Collins, 2006; p 763.

(34) Douda, B. E.; Blunt, R. M.; Bair, E. J. Visible Radiation from Illuminating-Flare Flames: Strong Emission Features*†. *J. Opt. Soc. Am.* **1970**, *60* (8), 1116.

(35) Koch, E. C.; Dochnahl, A. IR Emission Behaviour of Magnesium/Teflon/Viton (MTV) Compositions. *Propellants Explos. Pyrotech.* **2000**, *25* (1), 37–40.

(36) Sutton, W. H. Microwave Processing of Ceramic Materials. *Am. Ceram. Soc. Bull.* **1989**, *68* (2), 376–386.

(37) Menéndez, J. A.; Arenillas, A.; Fidalgo, B.; Fernández, Y.; Zubizarreta, L.; Calvo, E. G.; Bermúdez, J. M. Microwave Heating Processes Involving Carbon Materials. *Fuel Process. Technol.* **2010**, *91* (1), 1–8.

(38) Chen, J. Y.; Hsu, W. H.; Huang, C. L. Dielectric Properties of Magnesium Oxide at Microwave Frequency. *J. Alloys Compd.* **2010**, *504* (1), 284–287.

(39) Krupka, J.; Derzakowski, K.; Riddle, B.; Baker-Jarvis, J. A Dielectric Resonator for Measurements of Complex Permittivity of Low Loss Dielectric Materials as a Function of Temperature. *Meas. Sci. Technol.* **1998**, *9* (10), 1751–1756.

(40) Walkiewicz, J. W.; Kazonich, G.; McGill, S. L. Microwave Heating Characteristics of Selected Minerals and Compounds. In *AIME Transactions*; 1988; Vol. 284, p 4.